Author Accepted Manuscript version of the paper by Kang Qiu et al.
in Computer-aided chemical engineering, Vol 52 (2023) Page 1545-1550, DOI: http://dx.doi.org/10.1016/B978-0-443-15274-0.50246-8.
Distributed under the terms of the Creative Commons Attribution License (CC BY 4.0)

Model predictive control of compact combined cycles in offshore power plants integrating a wind farm

Kang Qiu [a], Leif E. Andersson [a*], Cristina Zotică [a], Adriana Reyes-Lúa [a], Rubén M. Montañés[a], Adriaen Verheyleweghen[b], Valentin Chabaud [a], Til Kristian Vrana [a]

[a] *SINTEF Energy Research, Sem Sælands vei 11, 7034 Trondheim, Norway*
[b] *Cybernetica AS, Leirfossvegen 27, 7038 Trondheim, Norway*
** Corresponding author: leif.andersson@sintef.no*

Abstract

Combined cycle gas turbine plants (CCGTs) fulfill an important role in emission reduction of offshore power systems as the bottoming cycle (BC) produces additional power from exhaust heat of the gas turbines (GTs). With increasing integration of wind turbines, CCGTs offshore must be flexible and provide variation management to the offshore energy system across multiple time scales. This work proposes a model predictive controller (MPC) sending setpoints to the CCGT to satisfy demand in the offshore power system under fluctuating wind power. A high-speed surrogate model suitable for optimizing in an MPC is identified. A linear MPC using a quadratic cost function with process constraints is formulated. The model-based control structure is then validated in simulation for satisfying a constant power demand under disturbances introduced by fluctuating wind power.

Keywords: Model predictive control; steam bottoming cycle; surrogate modelling; feedforward disturbance rejection; PI-control; wind power

1. Introduction

Currently, natural gas fueled gas turbines (GTs) are the main source of power in offshore oil and gas installations. National and international CO_2 reduction targets are incentivizing offshore operators to develop emission reduction strategies such as increasing energy efficiency and low emission power generation solutions like offshore wind power. It is likely that more than one technology will be implemented (Voldsund et al., 2023), resulting in a hybrid integrated offshore power generation system (Riboldi et al., 2020). In this work, we study a system with a combined cycle (CCGT) and power from wind. In CCGTs, the bottoming cycle (BC) uses the exhaust heat from GTs to produce additional power in a steam turbine (ST) and increase thermal energy efficiency (Nord and Bolland, 2013). Due to weight and space limitations, BCs on offshore installations are designed to be low weight and compact, which affects their dynamic response (Montañés et al., 2021). As simple cycle GTs, CCGTs offshore must provide variation management to the offshore energy system across multiple time scales, stabilizing the power generation system. Decentralized control strategies for compact BCs and CCGT based on PI- and feedforward controllers were studied by Nord and Montañés (2018), and model-based nonlinear feedforward in combination with PI-controllers was developed by Zotică et al. (2022).

Author Accepted Manuscript version of the paper by Kang Qiu et al.
in Computer-aided chemical engineering, Vol 52 (2023) Page 1545-1550, DOI: http://dx.doi.org/10.1016/B978-0-443-15274-0.50246-8.
Distributed under the terms of the Creative Commons Attribution License (CC BY 4.0)

The requirements for disturbance rejection of CCGTs are stringent when integrating non-dispatchable wind turbines to the power generation system offshore, due to the increased variability of the net load to be covered by the CCGT. A model predictive controller (MPC) is proposed to control the setpoints to the GTs and provide setpoints to the lower PID control layer of the BC by exploiting information, e.g., of the required system demand, wind profile forecasts, and a model of the disturbance. This enables the CCGT power output of the integrated system to minimize generation and consumption mismatches, thereby stabilizing the electrical frequency of the power system. Furthermore, the MPC framework allows for additional control objectives, such as minimizing CO_2 emissions and inherently handle steam temperature and pressure constraints.

2. System description and model

Figure 1 depicts the system considered in this work, consisting of an integrated wind-thermal electricity generation system. We assume that the thermal system should compensate for variations in wind power generation. The thermal system, a CCGT, consists of two GTs and a BC with two once-through steam generators (OTSG) connected to a common steam turbine (ST) and condenser system. A wind farm produces non-dispatchable power and the CCGT stabilizes the integrated power output. We simulate the power from the wind farm and CCGT using high-fidelity models and develop a surrogate model of the CCGT for the MPC.

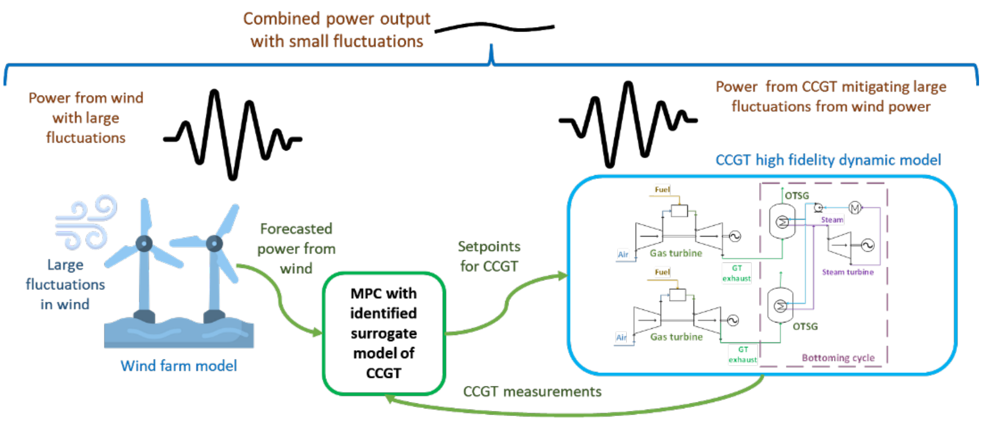

Figure 1. Conceptual description of the system.

2.1. Power from wind farm

The considered wind power plant consists of three wind turbines with 8 MW power rating each. The specifications are inspired by the Siemens Gamesa SG 8.0-167 DD wind turbine, but they do not represent that turbine in detail, as the details are not publicly available. The control of the wind turbines is taken as state-of-the-art grid-following maximum-power-point-tracking control, where the turbine actions are almost purely driven by the incoming wind, from which as much energy as possible is harvested. The wind turbines do not actively attempt to stabilize the electric power system. The task of stable control of the electric system is purely left to the gas turbines. This principle reflects the control of commercially available wind turbines, and the typical variation management strategy in wind-thermal systems (Burton, 2011).

Author Accepted Manuscript version of the paper by Kang Qiu et al.
in Computer-aided chemical engineering, Vol 52 (2023) Page 1545-1550, DOI: http://dx.doi.org/10.1016/B978-0-443-15274-0.50246-8.
Distributed under the terms of the Creative Commons Attribution License (CC BY 4.0)

The turbine layout is taken as a straight line with a spacing of ten diameters between turbines (standard, conservative spacing). A wind speed of 10 m/s with direction perpendicular to the layout (no wake) and with standard turbulence level is chosen. The incoming wind is then obtained from a farm-scale synthetic turbulence generator providing the rotor-averaged (power-equivalent) wind speed with consistent low-frequency fluctuations and correlation between turbines (Chabaud, 2023), for a consistent representation of wind power variability.

2.2. High fidelity dynamic model of the combined cycle

SINTEF Energy Research developed a high-fidelity dynamic Modelica model of the CCGT (Montañés et al., 2021; Zotică et al., 2022), using the commercial modeling and simulation environment Dymola. We utilize Modelica models from the Thermal Power Library 1.21 and adapt them to build up the combined cycle power plant models. In this work we model the thermo-hydraulics of the steam cycle of the CCGT with high-fidelity principles and apply a simplified quasi-static model for the GT based on data provided by Siemens Energy through the LowEmission Consortium. The bottoming cycle is based on the design presented in Zotică et al. (2022). For further details on the underlying models for turbine islands and steam generators, refer the work by Montañés et al. (2017) and Zotică et al. (2022). OTSG models are explained in the work by Montañés et al. (2021).

2.3. MPC surrogate model of the combined cycle

In this work, the surrogate model used for the predictive controller is a linear, autoregressive model of the CCGT predicting the steam turbine power output P_s, and CO_2 emissions from the operation of the GTs. The parameters of the surrogate model are determined with a stability-constrained linear regression performed on data gathered from simulation of the high-fidelity dynamic model of the CCGT.

The GT power x_{GT} and GT CO_2 emissions x_{CO_2} are modelled dependent on the current GT load, u_{GT},

$$x_{GT} = f(u_{GT}) \tag{1}$$

$$x_{CO_2} = f(u_{GT}). \tag{2}$$

The dynamics of the BC are highly nonlinear. However, the lower PID control layer results in more linearized dynamics (see section 3.1) and enables the use of a linear prediction model for the MPC. In the BC, the OTSG consists of relatively large volumes and mass of metal walls that accumulate heat over time. Hence, the BC exhibits high thermal inertia at the interface of the gas turbine exhaust and steam generation in the OTSG (Montañés et al., 2021). Therefore, the surrogate model necessitates a higher order, n, for modelling the predicted ST power in the next timestep $k+1$. The ST power is predicted from the temperature setpoints u_t and pressure setpoint u_p of the BC

$$x_{ST,k+1} = f\left(x_{BC,k-n}, u_{GT,k-n}, u_{t,k-n}, u_{p,k-n}\right),\ n = 0,..,5 \tag{3}$$

3. Control structure

The control structure proposed in this paper consists of a lower PID control layer of the BC and GT and an upper MPC control layer to provide setpoints to the lower layer.

3.1. PID control layer

The lower PID control layer keeps the superheated steam temperature at the outlet of the two OTSGs and superheated steam pressure at a setpoint given by the upper supervisory control layer (MPC). The power output of the ST is highly dependent on the enthalpy at

Author Accepted Manuscript version of the paper by Kang Qiu et al.
in Computer-aided chemical engineering, Vol 52 (2023) Page 1545-1550, DOI: http://dx.doi.org/10.1016/B978-0-443-15274-0.50246-8.
Distributed under the terms of the Creative Commons Attribution License (CC BY 4.0)

the inlet of the steam turbine. The BC heat input is mostly given by the gas turbine operation specified as GT load. The live steam pressure is controlled by manipulating the valve upstream the ST using a pure I-controller. The temperature is controlled by manipulating the feedwater flowrate, using a combination of model-based nonlinear feedforward for disturbance rejection and a feedback PI-controller to reject unmeasured disturbances and account for plant model mismatch. The nonlinear feedforward is derived from a simple steady-state energy balance over the OTSG. It receives measurements from the hot gas side flowrate and temperatures which are the main disturbances for the BC. The I and PI controllers are tuned from step responses using the SIMC tuning rules (Skogestad, 2003).

3.2. MPC control layer

The MPC provides GT setpoints u_{GT}, superheated steam temperature setpoints u_t, and the superheated steam pressure setpoint u_p to the lower PID control layer. A linear MPC using a quadratic cost function with input constraints, and the surrogate model described in 2.3 is formulated

$$
\begin{aligned}
&\min_{u} \ \omega_d J_d + \omega_{CO_2} J_{CO_2} + \omega_a J_a \\
&s.t. \ \ x_{k+1} = f(x_{k-n}, u_{k-n}),\ n = 0,..5,\ k = 0, \dots, N-1 \\
&\quad g(u_k) \le 0,\ \ k = 0,\ \dots, N-1 \\
&\quad x_0 = \hat{x}_0.
\end{aligned} \tag{4}
$$

The objective of the MPC consists of, in order priority, a power tracking cost J_d to satisfy a power demand, a CO_2 emission penalty J_{CO_2}, and an actuation cost J_a. The power tracking cost is calculated from the difference between the total predicted power output, consisting of the power output from the GTs x_{GT} and ST x_{ST}, forecasted wind power p_w, and the power demand p_d

$$J_d = \sum_{k=0}^{N} (p_{d,k} - p_{w,k} - x_{GT,k} - x_{ST,k})^2. \tag{5}$$

The CO_2 emission penalty is a quadratic cost on the predicted CO_2 emissions

$$J_{CO_2} = \sum_{k=0}^{N} x_{CO_2}{}^2. \tag{6}$$

Lastly, the actuation cost penalizes the change in the GT setpoints u_{GT}, BC temperature setpoints u_t, and BC pressure setpoint u_p with a quadratic cost

$$J_a = \sum_{k=0}^{N-1} (u_{GT,k+1} - u_{GT,k})^2 + (u_{t,k+1} - u_{t,k})^2 + (u_{p,k+1} - u_{p,k})^2. \tag{7}$$

To simplify the tuning of the weights ω, both the state and input variables are normalized to ensure comparability of the subobjectives J_{CO_2} and J_a. As J_d is the most important subobjective, the ω_d is set first. Afterwards ω_{CO_2} and ω_a are tuned by trial and error.

4. Results and discussion

The proposed MPC is tested in a simulation environment introduced in 4.1. The results (see 4.2) illustrate the disturbance rejection the MPC provides given fluctuating wind power and ST power output.

4.1. Simulation environment

The MPC is simulated in loop with a Gaussian process model of the CCGT regressed from data gathered from the high-fidelity model. The sampling time of 5 s and prediction horizon of 5 min were chosen to account for the vastly different time dynamics of the

Author Accepted Manuscript version of the paper by Kang Qiu et al.
in Computer-aided chemical engineering, Vol 52 (2023) Page 1545-1550, DOI: http://dx.doi.org/10.1016/B978-0-443-15274-0.50246-8.
Distributed under the terms of the Creative Commons Attribution License (CC BY 4.0)

GTs and the BC, which exhibited a closed loop settling time of 10^0-10^1 s and 10^2-10^3 s, respectively (Montañés et al., 2021). The simulation environment is assumed to provide full-state feedback of the ST power, GT power, and CO_2 emissions of the GTs. Realistic wind profiles as described in Section 2.1, assumed to be forecasted exactly, are utilized. The simulations are formulated with CasADi (Andersson et al., 2019) and solved with IPOPT (Wächter and Biegler, 2006), where each MPC iteration is solved within 0.05 s.

4.2. Results

Figure 2(a) shows the cumulative power output of the wind turbines and the CCGT. The proposed MPC can control the CCGT to provide variation management under fluctuating wind power to satisfy a constant demand of 70 MW. Figure 2(b), showing the relative power of the wind turbines, GTs, and ST scaled to the total power demand indicates that fluctuations in wind power are mainly compensated by the power output of the GTs due to their fast dynamics.

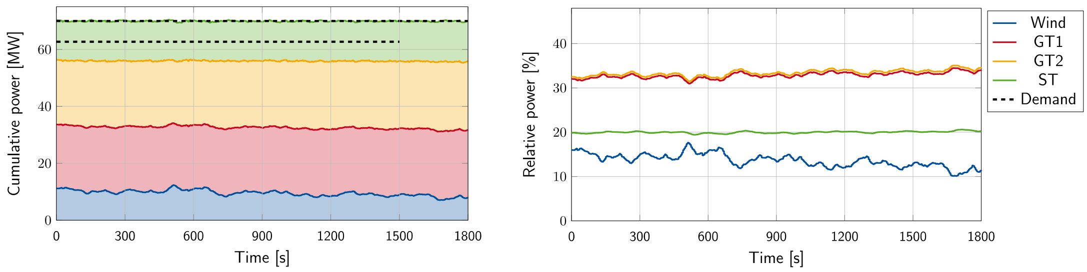

(a) (b)

Figure 2. (a) Cumulative power output of the combined wind-thermal system. (b) Relative power output of CCGT and wind scaled to total demand.

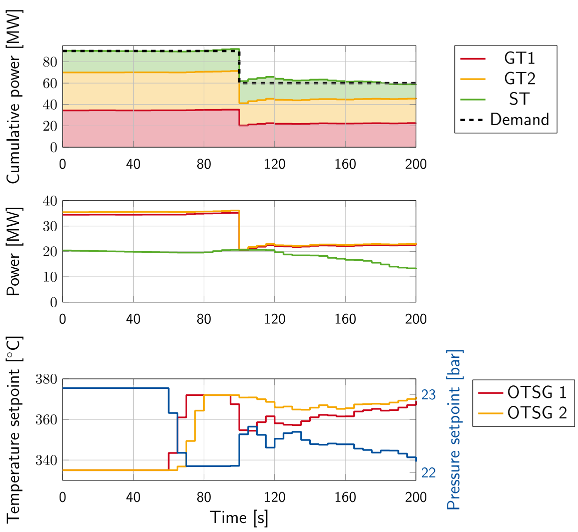

Figure 3. MPC step response showing cumulative power, GT load inputs, and steam temperature and pressure setpoints chosen by the MPC.

Figure 3 illustrates the working principle of the MPC when the power demand of the CCGT changes, e.g., due to a change in wind power or overall wind-thermal system demand. Overall, the CCGT responds sufficiently fast to the step change in power

Author Accepted Manuscript version of the paper by Kang Qiu et al.
in Computer-aided chemical engineering, Vol 52 (2023) Page 1545-1550, DOI: http://dx.doi.org/10.1016/B978-0-443-15274-0.50246-8.
Distributed under the terms of the Creative Commons Attribution License (CC BY 4.0)

demand. The GT loads are adjusted at time of demand change, as GTs have a fast dynamic response. Furthermore, the MPC accounts for the slower dynamic response of the BC by regulating the gas turbine loads at $t = 100\ s$ lower than the steady state gas turbine load at $t \geq 200\ s$.The dynamic response of the BC is improved by MPC as it regulates the setpoints to the lower PID control layer at $t = 60\ s$ before the demand step change at $t = 100\ s$ to account for the slower BC dynamics

5. Conclusion

This work proposes an MPC for CCGT control with variation management, and CO_2 emission reduction objectives. To formulate the MPC, a linear surrogate model is identified. As the CCGT process and the high-fidelity Modelica model are highly nonlinear, it is challenging to represent the dynamics correctly in a linear model.
Simulations show that the MPC helps to achieve variation management of the integrated wind-thermal system by controlling the CCGT under fluctuating, realistic wind profiles.
Further work should address uncertain wind profile forecasts and investigate different objectives to the MPC.
The MPC offers a flexible framework in realizing other control objectives for the offshore power system, which will be investigated.

Acknowledgements

This publication has been produced with support from the LowEmission Research Centre (www.lowemission.no), performed under the Norwegian research program PETROSENTER. The authors acknowledge the industry partners in LowEmission for their contributions and the Research Council of Norway (296207). We acknowledge SIEMENS Energy AG for providing the gas turbine model used as reference.

References

Andersson, J.A.E., Gillis, J., Horn, G., Rawlings, J.B., Diehl, M., 2019. CasADi: a software framework for nonlinear optimization and optimal control. Math. Prog. Comp. 11, 1–36. https://doi.org/10.1007/s12532-018-0139-4

Burton, T. (Ed.), 2011. Wind energy handbook, 2nd ed. ed. Wiley, Chichester, West Sussex.

Chabaud, V., 2023. Synthetic turbulence modelling for offshore wind farm engineering models using coherence aggregation (preprint). Preprints. https://doi.org/10.22541/au.167543645.56253178/v1

Montañés, R.M., Skaugen, G., Hagen, B., Rohde, D., 2021. Compact Steam Bottoming Cycles: Minimum Weight Design Optimization and Transient Response of Once-Through Steam Generators. Front. Energy Res. 9, 687248. https://doi.org/10.3389/fenrg.2021.687248

Nord, L.O., Bolland, O., 2013. Design and off-design simulations of combined cycles for offshore oil and gas installations. Applied Thermal Engineering 54, 85–91. https://doi.org/10.1016/j.applthermaleng.2013.01.022

Riboldi, L., Alves, E.F., Pilarczyk, M., Tedeschi, E., Nord, L.O., 2020. Optimal Design of a Hybrid Energy System for the Supply of Clean and Stable Energy to Offshore Installations. Front. Energy Res. 8, 607284. https://doi.org/10.3389/fenrg.2020.607284

Author Accepted Manuscript version of the paper by Kang Qiu et al.
in Computer-aided chemical engineering, Vol 52 (2023) Page 1545-1550, DOI: http://dx.doi.org/10.1016/B978-0-443-15274-0.50246-8.
Distributed under the terms of the Creative Commons Attribution License (CC BY 4.0)

Skogestad, S., 2003. Simple analytic rules for model reduction and PID controller tuning. Journal of Process Control 13, 291–309. https://doi.org/10.1016/S0959-1524(02)00062-8

Voldsund, M., Reyes-Lúa, A., Fu, C., Ditaranto, M., Nekså, P., Mazzetti, M.J., Brekke, O., Bindingsbø, A.U., Grainger, D., Pettersen, J., 2023. Low carbon power generation for offshore oil and gas production. Energy Conversion and Management: X 17, 100347. https://doi.org/10.1016/j.ecmx.2023.100347

Wächter, A., Biegler, L.T., 2006. On the implementation of an interior-point filter line-search algorithm for large-scale nonlinear programming. Math. Program. 106, 25–57. https://doi.org/10.1007/s10107-004-0559-y

Zotică, C., Montañés, R.M., Reyes-Lúa, A., Skogestad, S., 2022. Control of steam bottoming cycles using nonlinear input and output transformations for feedforward disturbance rejection. IFAC-PapersOnLine 55, 969–974. https://doi.org/10.1016/j.ifacol.2022.07.570